CrystEngComm

PAPER

View Article Online
View Journal

A Zn azelate MOF: combining antibacterial effect†

Cite this: DOI: 10.1039/c4ce00885e

C. Tamames-Tabar,[ab] E. Imbuluzqueta,[a] N. Guillou,[b] C. Serre,[b] S. R. Miller,‡[b] E. Elkaïm,[c] P. Horcajada§*[b] and M. J. Blanco-Prieto§*[a]

Received 26th April 2014,
Accepted 13th June 2014

DOI: 10.1039/c4ce00885e

www.rsc.org/crystengcomm

A novel biocompatible and bioactive Metal–Organic Framework (BioMOF), named BioMIL-5 (Bioactive Materials from Institut Lavoisier), was hydrothermally synthesized from a Zn^{2+} salt and azelaic acid, both with interesting antibacterial and dermatological properties. Its structure was determined by high resolution X-ray powder diffraction, and further characterized by infrared spectroscopy, thermogravimetric analysis and elemental analysis. The determination of the minimal inhibitory concentration (MIC) and minimal bactericidal concentration (MBC) values of BioMIL-5 in *Staphylococcus aureus* and *Staphylococcus epidermidis* demonstrated that the antimicrobial activity of the individual components of BioMIL-5 were maintained after its synthesis. Moreover, BioMIL-5 was found to be stable in water and in bacterial culture medium, especially in water, leading to the subsequent progressive release of its active constituents, AzA and Zn^{2+} ions. Interestingly, this slow active delivery allowed control of the growth of a *S. epidermidis* suspension over 7 days. The high stability of this material and the maintenance of its antibacterial properties make BioMIL-5 a good candidate for future bioapplications, for skin care and in cosmetics.

Introduction

Metal–Organic Frameworks (MOFs) are a very versatile group of crystalline hybrids, due to their broad application fields, including catalysis, and separation or gas storage, among others.[1] Although their first potential applications were mainly focused on these fields, in recent years, MOFs have also been directed towards biomedicine.[2] These have been evaluated as new controlled delivery systems for drugs,[2a,3] cosmetics,[4] or biologically active gases,[5] encapsulation of enzymes[6] and finally for imaging[7] and theranostics.[3a,8]

MOFs can work as drug controlled-release carriers by (i) entrapping the active molecule within their porosity[3–6] or by (ii) incorporating the biomolecule as a constitutive part of their skeleton.[2b,9] In this latter case, these are also known as BioMOFs (Bioactive Metal–Organic Frameworks). This latter strategy permits the use of therapeutically active molecules bearing multiple complexing groups, as well as bioactive cations (Ca^{2+}, $Fe^{2/3+}$, Ag^{+}, Zn^{2+}), to build the BioMOF and then deliver the active compounds *via* framework degradation.[10] While the best antibacterial activity has been validated for antibacterial–metal molecular complexes by combining different antibiotic drugs and metals,[11] to the best of our knowledge, no studies dealing with such combinations have been published about MOFs. Indeed, studies reporting the antibacterial activity of MOFs are typically based on non-toxic antimicrobial cations (Zn^{2+},[12] Ag^{+},[10a,13]).

In particular, Zn^{2+} is an endogenous low-toxic transition metal cation[14] widely used in dermatology, as a cicatrizing agent and skin moisturiser with antidandruff, astringent, anti-inflammatory and antibacterial properties,[15] but without controlled release.

On the other hand, azelaic acid (nonanedioic acid or AzA) exhibits antibacterial[16] and anti-inflammatory[17] properties and is regularly used as a routine treatment against acne vulgaris[18] and rosacea.[19] AzA has shown a great potential for the treatment of other skin pathologies such as malignant melanoma,[20] hyperpigmentation[21] and melasma.[22] However, it is poorly absorbed through the skin and requires several applications to maintain active levels for an extended period.[23]

The combination of AzA and Zn^{2+} into a robust MOF would result into long drug release carriers. The development

[a] *Department of Pharmacy and Pharmaceutical Technology, School of Pharmacy, University of Navarra, Irularrea 1, 31008 Pamplona, Spain. E-mail: mjblanco@unav.es; Fax: +34 948425649; Tel: +34 948425600 ext. 806519*

[b] *Institut Lavoisier, UMR CNRS 8180, Université de Versailles Saint-Quentin-en-Yvelines, 45 Avenue des Etats-Unis, 78035 Versailles Cedex, France. E-mail: patricia.horcajada-cortes@uvsq.fr; Fax: +33(0) 139254452; Tel: +33(0) 139254371*

[c] *Cristal beamline, Soleil Synchrotron, L'Orme des Merisiers Saint Aubin, BP4891192 Gif-sur-Yvette Cedex, France*

† Electronic supplementary information (ESI) available: Crystallographic details, physicochemical characterisations (TGA, XRPD, XRTD and SEM) and degradation studies. See DOI: 10.1039/c4ce00885e

‡ Present address: UOP Research Center, UOP LLC, a Honeywell Company, 25 East Algonquin Road, Des Plaines, Illinois 60017, USA.

§ PH and MJBP are equal senior authors.

of such drug delivery systems could contribute to major technological progress for future bioapplications in dermatology and skin care.

In the present study, we report the synthesis of a new BioMOF, named BioMIL-5 (MIL stands for Materials of Institut Lavoisier), based on Zn^{2+} ions as inorganic nodes and AzA as the organic linker, both with very interesting properties for the dermatological treatment of various skin disorders. First, its structure was determined by means of high resolution X-ray powder diffraction data, further confirmed by physico-chemical characterizations. The release of its active constitutive compounds was also assessed by stability tests of BioMIL-5 in water and in bacteria broth at 37 °C. Finally, the antibacterial activity of BioMIL-5 was evaluated by using 2 common Gram-positive bacteria normally found in skin (*S. aureus* and *S. epidermidis*).

Experimental section

Chemicals and reagents

Zinc nitrate hexahydrate ($Zn(NO_3)\cdot 6H_2O$) and azelaic acid (AzA) were purchased from Sigma-Aldrich (Germany). All solvents, absolute ethanol (EtOH) and nitric acid 37% (HNO_3 37%) were acquired from Carlo Erba (Italy), except for the high performance liquid chromatography (HPLC) grade acetonitrile (AcN) and dimethyl sulfoxide (DMSO) acquired from Merck KGaA (Germany). AzA-derivatization was accomplished using 4-bromophenacyl bromide and *N*,*N*-diisopropylethylamine, both purchased from Sigma-Aldrich (Germany) and ammonium formate (NH_4HCO_2) purchased from AVOCADO Research Chemical Ltd. (UK). The Zn standard for atomic absorption spectroscopy 1 mg mL^{-1} Zn in nitric acid TraceCERT® was purchased from Fluka (Switzerland). Both Mueller-Hinton cation adjusted broth (MHCA) and trypticase soy agar (TSA) were purchased from Becton Dickinson and Company (USA).

BioMIL-5 synthesis and characterisation

BioMIL-5 synthesis: 297 mg of $Zn(NO_3)\cdot 6H_2O$ (1 mmol) together with 47 or 188 mg of AzA (0.25 or 1 mmol) and 5 mL of MilliQ water were put inside a 23 mL Teflon Parr Bomb (Parr Instrument Company, USA) and incubated for 24 h at 200 °C in a Heraeus Oven (Thermo Scientific, USA) with a ramp to temperature of 1 h. Then, the particles were recovered by filtration and washed with water. Initial conditions based on a Zn : AzA stoichiometry of 1 : 0.25 led to a good crystalline solid used for structural determination but with the presence of a ZnO impurity.

Optimized synthetic conditions, based on a Zn : AzA stoichiometry equal to 1 : 1, yielded a pure BioMIL-5. The amount of recovered solid was approximately 150 mg (yield ~52%).

Structural determination

No suitable single crystal with a sufficient size or quality for a structural investigation was available. High resolution X-ray powder diffraction data were then collected on the CRISTAL beamline at Soleil Synchrotron (Gif-sur-Yvette, France). A monochromatic beam was extracted from the U20 undulator beam by means of a Si(111) double monochromator. Its wavelength of 0.72528 Å was refined from a LaB_6 (NIST Standard Reference Material 660a) powder diagram recorded prior to the experiment. High angular resolution was obtained with, in the diffracted beam, a 21 perfect crystal Si(111) multi-analyzer similar to the one employed on beamline ID31 at ESRF.[24] The sample was loaded in a 0.7 mm capillary (Borokapillaren, GLAS, Schönwalde, Germany) mounted on a spinner rotating at about 5 Hz to improve the particles' statistics. Diffraction data were collected for less than 2 h in continuous scanning mode and the diffractogram was obtained from the precise superposition and addition of the 21 channels data.

Extractions from the peak positions, pattern indexing, Fourier difference calculations and Rietveld refinements were carried out with the TOPAS program.[25] Structural determination was performed with the EXPO package,[26] using EXTRA for extracting integrated intensities and SIR97 for direct-method structure solutions. 31 restraints on Zn–O, C–C and C–O distances were applied in order to maintain a suitable geometry during the refinement.

Fourier Transformed Infrared Spectroscopy (FTIR) was performed on a Thermo Nicolet 6700 spectrometer (Thermo, USA) registering the spectra at a wavelength interval of 4000–400 cm^{-1} at RT. Thermogravimetric analyses (TGA) were carried out using a Perkin Elmer Diamond STA 6000 apparatus (Perkin Elmer, USA) under oxygen gas with a heating rate of 3 °C min^{-1}. Morphologic analysis of the crystals was carried out with a field-emission gun scanning electron microscope (FEG-SEM) JEOL JAMP 9500F (JEOL GmbH, Germany), dynamic light scattering (DLS) measurements with a Mastersizer S® (Malvern Instruments, UK).

BioMIL-5 degradation and release of AzA and Zn

For the BioMIL-5 degradation study and AzA and Zn^{2+} release monitoring, 1 mL of media (water or MHCA broth) was added to 4.3 mg of solid and kept inside an incubator under rotational stirring at 37 °C during 70 days. After different incubation times, the samples were removed from the incubator and centrifuged (14 100*g*/15 min). The pellet was characterized by means of FTIR, XRPD, SEM and DLS. The released amount of AzA and Zn was quantified in the sample supernatant by high performance liquid chromatography (HPLC) and atomic absorption spectroscopy (AAS), respectively. The solubility values of AzA in both media at 37 °C were experimentally determined as 2.2 and 3.4 mg mL^{-1} for water and MHCA, respectively.

Quantification of AzA. AzA released from BioMIL-5 was analysed after its derivatization by an HPLC system (Waters Alliance C2695) coupled to a photodiode array detector (PAD) (Waters E2998) and controlled by Empower software (Version 5.00, Waters Corporation, USA). The derivatization was

carried out by a previously described method[27] with minor modifications. Briefly, 1 mL of supernatant was added to 500 μL of 4-bromophenacyl bromide (50 mg mL^{-1} in AcN) and 200 μL of *N*,*N*-diisopropylethylamine. After their vortex mixing, samples were incubated at 60 °C during 30 min and analyzed by HPLC.

The chromatographic separation was carried out using a Durashell C18 column (5 μm, 150 mm × 4.6 mm I.D., Agela Technologies Inc., USA) protected by a guard cartridge precolumn with the same packing material. For all the samples, an isocratic elution profile was established and the flow rate was set at 1 mL min^{-1}. The mobile phase composition varied depending on the sample type, being 80% of AcN and 20% of NH_4HCO_2 1 M (pH = 5) for water samples and 50% of AcN and 50% of NH_4HCO_2 1 M (pH = 5) for MHCA broth samples. The injection volume was 20 μL and AzA was detected by UV absorbance at the wavelength of 250 nm. The standard curve was prepared by dilutions of a 1 mg mL^{-1} AzA mother solution in AcN.

Quantification of Zn. The Zn^{2+} content of the samples was analyzed using a Thermo Electron Corporation M Series atomic absorption spectrometer (Thermo Scientific, USA) with a Zn lamp at 213.9 nm using SOLAAR software (Thermo Scientific, USA). Samples were diluted 1 : 100 (in water/MHCA depending on the sample type) prior to analysis and the calibration curve was prepared by dilutions of the Zn^{2+} standard in HNO_3 2%.

Antibacterial activity studies

Antibacterial properties of the synthesized BioMIL-5 were evaluated against *Staphylococcus aureus* ATCC (American Type Culture Collection) 25923 and *Staphylococcus epidermidis* ATCC 12228. Experiments were performed with fresh bacteria previously incubated on TSA plates at 37 °C for 24 h.

First, minimal inhibitory concentration (MIC) and minimal bactericidal concentration (MBC) values for BioMIL-5 and its individual components (AzA and Zn) were determined in MHCA broth by broth microdilution method according to the CLSI recommendations.[28] Experiments were carried out by suspending BioMIL-5 in these media at 37 °C, as well as the equivalent amounts of its individual components (1.1 and 3.2 mg, for Zn and AzA, per 4.3 mg of BioMIL-5 respectively). Briefly, stock concentrations of BioMIL-5, as well as the corresponding amounts of their constitutive ligand and metal (AzA and Zn), were prepared in 0.9% saline solution and further diluted in MHCA broth to different concentrations. Bacterial suspensions in 0.9% saline solution were adjusted to an optical density of 0.085 (600 nm) (~10^8 colony forming units (CFU) mL^{-1}) with a Thermo Scientific Genesys 20 Spectrophotometer (Thermo Scientific, USA) and diluted 1 : 100 in MHCA broth. The real inoculum was determined by plating appropriate dilutions on TSA plates. Finally, 100 μL of each treatment were mixed with 100 μL of each bacterial suspension in 96-well plates resulting in final treatment concentrations ranging from 0.031 to 6 mg mL^{-1}. As a control for bacterial growth, treatment-free medium was also included. After incubation at 37 °C for 24 h, MICs were defined as the lowest concentration of drug that resulted in no visible bacterial growth. For MBC determination, aliquots of 20 μL from the wells without visual bacterial growth were plated on TSA plates and incubated for 24 h at 37 °C. The minimum concentration that yielded more than 99.9% killing of the bacteria was defined as the MBC of each treatment.

On the other hand, in order to study the antibacterial properties of BioMIL-5 over time, a *S. epidermidis* suspension in MHCA broth (5×10^5 CFU mL^{-1}) was exposed to increasing concentrations of the BioMOF (0.9, 1.7 and 4.3 mg mL^{-1}) and bacterial growth was monitored at 37 °C and kept under stirring during 7 days. For comparing the previous results, the growth of non-treated bacteria was also monitored. At different incubation times, 100 μL of each bacterial suspension were plated on TSA plates for colony counting. Results of CFU counts were transformed into logarithms and represented *vs.* time to obtain the bacterial growth curves.

Results and discussion

BioMIL-5 synthesis and characterisation

White-shining thin platelet-shaped crystals (5–10 μm, with a few larger ones of around 30 μm) of the zinc azelate BioMIL-5 were initially prepared using a hydrothermal route and a Zn : AzA stoichiometry of 1 : 0.25. BioMIL-5 crystallises in the orthorhombic unit cell (a = 47.288(1), b = 4.7297(2), c = 9.3515(3) Å; V = 2091.5(1) $Å^3$). Systematic absences were consistent with the *Pcca* space group (no. 54). Unindexed lines observed on the powder pattern correspond to ZnO impurity due probably to the large excess of the Zn precursor (Zn : AzA = 1 : 0.25). Its structural model was introduced in the next steps of the structural investigation. Direct methods calculations allowed location of one independent zinc atom with most of its environment with few carbons. This structural model was completed by successive difference Fourier calculations. At the final stage, Rietveld refinement for BioMIL-5 involved the following structural parameter: 45 atomic coordinates, 1 overall thermal factor and the scale factor. The anisotropic line broadening effect was modelled by using spherical harmonics and soft restraints were maintained on bond lengths and angles. The final Rietveld plot (Fig. S1†) corresponds to satisfactory crystal structure model indicator (R_{Bragg} = 0.029) and profile factors (R_P = 0.076 and R_{WP} = 0.104). The amount of ZnO was estimated at about 5 wt% (weight). The unit cell contains one independent Zn atom located in a general position and two independent organic moieties located on a mirror, leading to the chemical formula $Zn(C_9O_4H_{14})$. Crystallographic data are summarized in Table S1.†

This structure is very close to the one of the cobalt pimelate MIL-36 or $(Co(C_7H_{10}O_4))$.[29] Similar structures have been more recently reported based on a cobalt adipate

($Co(C_6H_8O_4)$) or a zinc glutarate ($Zn(C_5H_6O_4)$).[30] Each Zn atom is tetrahedrally coordinated by oxygen atoms coming from the carboxylate groups of 4 azelate ligands. This leads to an infinite grid in the (011) plane of ZnO_4 tetrahedra linked by bridging CO_2^- groups (see Fig. 1). The connection along the [100] direction is insured by the aliphatic chains giving rise to the neutral 3-D framework of BioMIL-5. Therefore, a non-porous framework is generated, with a clear segregation of the hydrophilic (carboxylate + Zn) and hydrophobic part (alkyl chains). The shortest C···C distances between adjacent walls are 3.65(1) Å and 4.04(2) Å, respectively, suggesting a rather close packing of the long alkyl chains of the azelate ligand.

In order to prevent the formation of the ZnO impurity, synthetic conditions were further optimized by increasing the Zn : AzA ratio from 1 : 0.25 to 1 : 1. Thus, white-shining platelet-shaped crystals (10 ± 6 μm; Fig. 2) of the pure zinc azelate BioMIL-5 were successfully synthesized using a biocompatible and green hydrothermal route, avoiding the use of any toxic additive. XRPD confirmed the identity and the purity of the whole polycrystalline product (Fig. 3).

TGA analysis showed the absence of any residual solvent as well as only one weight loss of 67.2 wt% at around 320 °C, corresponding to the combustion of the azelate ligand (Fig. S2†), in agreement with the proposed structural formula (ZnO theo. = 32.3 wt%; calc. = 32.8 wt%).

FTIR spectrum of the BioMIL-5 showed the presence of ν(C–O) at 1450 and 1550 cm^{-1}. In addition, the absence of the ν(C═O) band at 1700 cm^{-1} confirmed the absence of free-remaining azelaic ligand (Fig. S4†).

Thermal stability of BioMIL-5 under air atmosphere reached 300 °C, as indicated by X-ray powder thermodiffraction patterns, in agreement with TGA (Fig. S3†).

BioMIL-5 degradation and release of AzA and Zn

In order to assess whether BioMIL-5 will be able to progressively release its therapeutic constitutive molecules (Zn and AzA), the BioMIL-5 degradation was studied in two different media: (i) MilliQ water for simulating skin conditions and (ii) MHCA bacteria broth, a more complex medium composed by many organic and inorganic nutrients (among them amino acids, sugars, casein, inorganic salts, *etc.*).[31] This last medium will be further used to evaluate the MIC and MBC values (see Results and discussion, Antibacterial activity studies). Experiments were carried out suspending 4.3 mg mL^{-1} of BioMIL-5 in these media at 37 °C. The degradation and subsequent release of AzA and Zn^{2+} from BioMIL-5, was monitored by analyzing both supernatant and pellet at different incubation times (see Experimental section). Degradation is represented as the wt% of the linker released in the medium, considering 100% as the total degradation of the BioMOF that is when the entire amount of linker and metal that build the particles is released to the medium.

As can be seen in Fig. 4, a perfect correlation was found between the degradation values obtained from the Zn^{2+} or AzA release in water (*i.e.* release of 6.9 ± 0.0 and 8.3 ± 0.3% after 7 days or 56.6 ± 3.9 and 51.4 ± 0.1% after 70 days for Zn and AzA, respectively). On the other hand, a slight difference between the degradation values estimated from either the Zn^{2+} or AzA release in the MHCA broth medium was observed (*i.e.* release of 14.8 ± 0.2 and 30.5 ± 0.0% after 7 days or 100.8 ± 0.1 and 92.3 ± 0.0% after 70 days for Zn and AzA, respectively). This might be related to the presence of

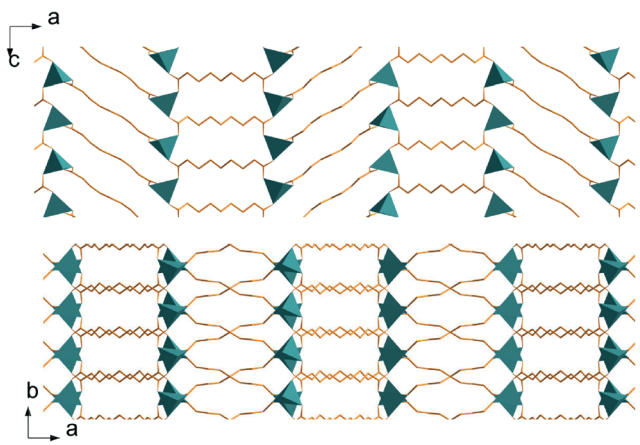

Fig. 1 Projections of the crystal structure of BioMIL-5 along [010] and [001] directions. Zn polyhedra and carbon atoms are in green and yellow, respectively.

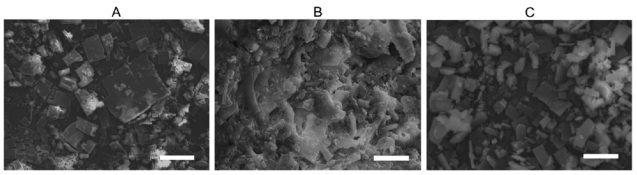

Fig. 2 SEM images of BioMIL-5 after synthesis (A), and after 70 days in Mueller Hinton Cation Adjusted broth or MHCA (B) and in water (C). The scale bar for all images is 10 μm.

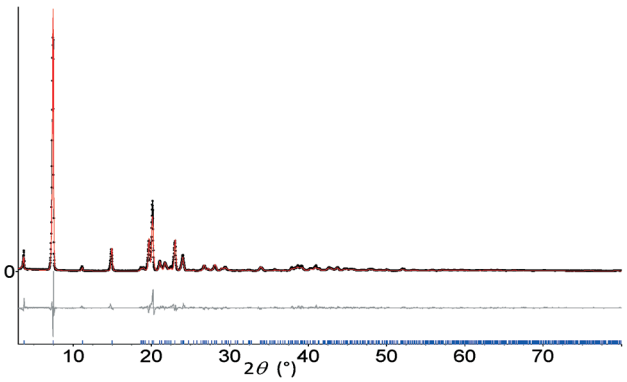

Fig. 3 Comparison of experimental (black points) and calculated (red line) patterns of BioMIL-5, confirming the purity of the solid. Laboratory X-ray powder diffraction data were collected on a Siemens D5000 diffractometer by using CuKα radiation. The pattern was scanned over an angular range 3–80° (2θ) with a step length of 0.02° (2θ).

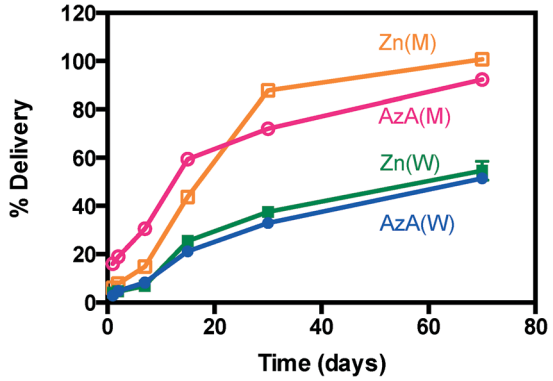

Fig. 4 Delivery profile of azelaic acid (AzA) and zinc (Zn) in Mueller Hinton cation adjusted broth or MHCA (M) and in water (W): AzA(M) (pink), AzA(W) (blue), Zn(M) (orange) and Zn(W) (green).

components in the medium able to interact differently with the AzA and Zn^{2+} complexes.

As can be observed in Fig. 4, BioMIL-5 degrades slowly and progressively in both media, the release in water being even slower than in MHCA broth. For instance, the degradation in water was found to be ~8 and ~55% after respectively 7 and 70 days of incubation, whereas in MHCA broth, the degradation was ~25 and ~95% after 7 and 70 days, respectively. The higher pH value obtained in MHCA in comparison with its value in MilliQ water (7.4 *vs.* 6.0), was several units above the pK_a of the azelate ligand (pK_a = 4.55 and 5.41),[32] and might favor the formation of Zn oxide/hydroxide and therefore, the degradation of the solid.[33] In addition, the presence of several amino acids, sugars and salts, in particular some phosphate groups (present in the MHCA broth composition for casein hydrolysis)[31] able to compete for the coordination of the Zn^{2+} cation with the azelate ligand, might explain the faster degradation of BioMIL-5 in MHCA. This fact is in total concordance with that already seen in other metal carboxylate MOFs when exposed to phosphate buffered saline.[3b,34]

In this sense, FTIR spectra (Fig. S5†) show an important intensity decrease on the bands at around 1450 and 1550 cm^{-1}, corresponding to the carboxylate bonds, as well as the presence of traces of free carboxylic acid bands (ν(C═O)) at around 1700 cm^{-1}. These results, together with the appearance of new bands at 1000 cm^{-1}, which can be assigned to ν(P═O) bands, are in complete agreement with the degradation of BioMIL-5 in MHCA medium.

Furthermore, in both media, the BioMIL-5 was not fully degraded during the degradation process, as confirmed by the XRPD patterns depicted in Fig. S4.† Whereas BioMIL-5 did not show any significant variation even after 70 days of immersion in water, confirming the high stability, an important Bragg peak broadening was observed after 70 days in MHCA broth medium, consistent with a larger extent of degradation. Interestingly, despite the progressive degradation of BioMIL-5 in MHCA broth, with around 95% of their constitutive parts released to the medium, the small amount of remaining solid stays crystalline up to the end of the assay. The important stability of BioMIL-5 contrasts with other previously reported zinc dicarboxylates, such as the well-known MOF-5.[35] This is due both to the absence of pores in BioMIL-5 and its hydrophobic character.[36]

Moreover, the morphological study showed that contrary to the large and polydispersed well-faceted crystals of the BioMIL-5 sample (9.83 ± 6.12 μm), SEM images after degradation showed smaller more or less rounded-corners crystals after 70 days of degradation in water (3.00 ± 0.02 and 1.83 ± 1.17 μm; Fig. 2). Note that for the BioMIL-5, very little solid was obtained after the degradation in MHCA, reflecting almost complete degradation. In accord with the SEM images, the particle sizes obtained by DLS measurements, for BioMIL-5 before and after 70 days immersed in water and in MHCA broth were 6.00 ± 3.50, 5.80 ± 0.45 and 0.78 ± 0.02 μm, respectively (note the important polydispersity of the sample, in agreement with the SEM observations, as well as the DLS measurement complexity considering the non-spherical form of the particles). This is consistent with the much higher degree of degradation of BioMIL-5 in MHCA broth than in water.

In light of these findings, one can presumably propose a degradation mechanism of BioMIL-5 in MHCA broth by erosion, in which the constitutive parts that are located on the external surface of the crystal are progressively released to the media, leading to a decrease in the crystal dimension without affecting the integrity of the crystalline framework.

Antibacterial activity studies

The antibacterial activity of BioMIL-5, as well as of its constituents (Zn and AzA), was first investigated by means of their MIC/MBC (MIC = Minimal Inhibitory Concentration; MBC = Minimal Bactericidal Concentration) determination against two Gram-positive bacteria present in the normal skin flora but which cause some skin disorders: *S. aureus* and *S. epidermidis* (see Experimental section).

MIC values for Zn, AzA and BioMIL-5 were 0.5, 1.5 and 1.7 mg mL^{-1}, respectively, and MBC values were 2.0, 3.0 and 4.3 mg mL^{-1}, respectively (Table 1). It is noteworthy that the biological activity of the original components of BioMIL-5 was maintained, not only after the hydrothermal synthesis conditions but also after the degradation of the hybrid network, releasing both Zn^{2+} and AzA in their active forms.

Table 1 Minimal inhibitory concentration (MIC) and minimal bactericidal concentration (MBC) results in mg mL^{-1} of azelaic acid (AzA), BioMIL-5 and Zn^{2+} in *S. aureus* and *S. epidermidis*

	S. aureus		*S. epidermidis*	
Treatment	MIC	MBC	MIC	MBC
BioMIL-5	1.7	4.3	1.7	4.3
AzA	1.5	3.0	1.5	3.0
Zn^{2+}	0.5	—	0.5	2.0

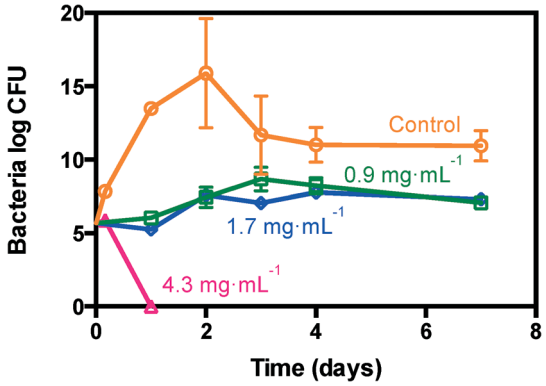

Fig. 5 Bacterial growth curves comparing the control group (orange) with BioMIL-5 at different concentrations (mg mL^{-1}): 0.9 (green), 1.7 (blue) and 4.3 mg mL^{-1} (pink) after 1 week in *S. epidermidis*.

Some comments can be proposed regarding the MBC values. Although an antibacterial additive effect between AzA and Zn^{2+} could be expected by their combination in BioMIL-5, no evidence supporting any synergistic activity was found. However, considering the different biological properties of AzA and Zn^{2+}, acting at different skin care levels (*i.e.* cicatrizing, antidandruff, astringent, anti-acne, *etc.*), one could rationally expect, that by simultaneously targeting different pathophysiological events, the AzA and Zn^{2+} released from BioMIL-5, might provide complementary beneficial actions in the treatment of skin disorders.

After determining the MIC/MBC values, the following step was to evaluate the influence of the slow release of both AzA and Zn^{2+} on the duration of the pharmacological effect of BioMIL-5. Therefore, the growth of a *S. epidermidis* suspension was monitored for 7 days in the absence or presence of three different BioMIL-5 concentrations (0.9, 1.7 and 4.3 mg mL^{-1}), in order to evaluate whether it had a time- or dose-dependent antibacterial profile. As depicted in Fig. 5, the presence of BioMIL-5 at the MIC (1.7 mg mL^{-1}) but more interestingly at 0.5 × MIC (0.9 mg mL^{-1}), significantly reduced the growth rate of *S. epidermidis* and stopped it after 48 h of incubation, evidencing a concentration-dependent biological activity of BioMIL-5. At 48 h, the number of CFU mL^{-1} was 7.76×10^{15} for the non-treated control and 2.82×10^{7} for bacteria treated with 0.9 mg mL^{-1} of BioMIL-5, evidencing a bacteriostatic effect. In addition, a bactericidal effect was observed at 24 h when treating the bacteria with 4.3 mg mL^{-1} (MBC), an effect that was maintained until the end of the study. Considering the BioMOF degradation, one can estimate a delivery of 0.2 mg mL^{-1} of each Zn^{2+} and AzA from BioMIL-5 (4.3 mg mL^{-1}) to the MHCA broth after 1 day. A bactericidal effect was achieved at much lower concentrations of BioMIL-5 (Fig. 5) than the MIC and MBC values established for the isolated Zn^{2+} and AzA components (Table 1), suggesting an additive effect between the Zn^{2+} and the azelate.

Conclusions

A new bioactive MOF material (BioMIL-5) was hydrothermally synthesized based on Zn^{2+} and AzA, and its structure was fully characterized. Both components exhibit interesting antibacterial and dermatological properties, and are currently being used for the treatment of several skin disorders and in the cosmetic industry.

Remarkably, the progressive release of the active Zn^{2+} and AzA from BioMIL-5, in both water and bacterial culture media, led to interesting and time-maintained antibacterial properties when used for 7 days against *S. epidermidis*, a Gram-positive bacterium.

Finally, the incorporation of BioMIL-5 in more complex formulations (*i.e.* semisolid pharmaceutical dosage forms such as creams or gels) by controlling its particle size or its external surface functionalization could improve its adhesion/penetration in various surfaces (*i.e.* skin, bacteria and other materials) and enhance its efficacy against a broader spectrum of bacteria.

Acknowledgements

Authors would like to acknowledge T. Devic, C. Thouvenot, T. Baati, L. Frizza and F. Bridoux for their help in XRD, AAS, HPLC and SEM characterisations. The authors thank Soleil for providing access to the beamline Cristal. C.T.T. would like to thank Asociación de Amigos de la Universidad de Navarra for the predoctoral grant. This work was partially supported by FeUN (Fundación Empresa Universidad de Navarra). Authors acknowledge the CNRS funding, the French ANR 2010-MatePro VirMIL and the EU funding ERC-2007-209241-BioMOFs.

Notes and references

1 See Themed Issues: (*a*) *Chem. Soc. Rev.*, 2009, **38**, 1201; (*b*) *Chem. Rev.*, 2012, **112**, 613.
2 (*a*) P. Horcajada, R. Gref, T. Baati, P. K. Allan, G. Maurin, P. Couvreur, G. Férey, R. E. Morris and C. Serre, *Chem. Rev.*, 2012, **112**, 1232; (*b*) F. Novio, J. Simmchen, N. Vázquez-Mera, L. Amorín-Ferré and D. Ruiz-Molina, *Coord. Chem. Rev.*, 2013, **257**, 2839; (*c*) J. Della Rocca, D. Liu and W. Lin, *Acc. Chem. Res.*, 2011, **44**, 957.
3 (*a*) P. Horcajada, C. Serre, M. Vallet-Regí, M. Sebban, F. Taulelle and G. Férey, *Angew. Chem., Int. Ed.*, 2006, **45**, 5974; (*b*) P. Horcajada, T. Chalati, C. Serre, B. Gillet, C. Sebrie, T. Baati, J. F. Eubank, D. Heurtaux, P. Clayette, C. Kreuz, J.-S. Chang, Y. K. Hwang, V. Marsaud, P.-N. Bories, L. Cynober, S. Gil, G. Férey, P. Couvreur and R. Gref, *Nat. Mater.*, 2010, **9**, 172.
4 D. Cunha, M. Ben Yahia, S. Hall, S. R. Miller, H. Chevreau, E. Elkaïm, G. Maurin, P. Horcajada and C. Serre, *Chem. Mater.*, 2013, **25**, 2767.
5 (*a*) N. J. Hinks, A. C. McKinlay, B. Xiao, P. S. Wheatley and R. E. Morris, *Microporous Mesoporous Mater.*, 2010, **129**, 330;

(*b*) B. Xiao, P. S. Wheatley, X. Zhao, A. J. Fletcher, S. Fox, A. G. Rossi, I. Megson, S. Bordiga, L. Regli, K. M. Thomas and R. E. Morris, *J. Am. Chem. Soc.*, 2007, **129**, 1203.

6 (*a*) V. Lykourinou, Y. Chen, X.-S. Wang, L. Meng, T. Hoang, L.-J. Ming, R. L. Musselman and S. Ma, *J. Am. Chem. Soc.*, 2011, **133**, 10382; (*b*) W.-L. Liu, S.-H. Lo, B. Singco, C.-C. Yang, H.-Y. Huang and C.-H. Lin, *J. Mater. Chem. B*, 2013, **1**, 928.

7 (*a*) W. J. Rieter, K. M. L. Taylor, H. An, W. Lin and W. Lin, *J. Am. Chem. Soc.*, 2006, **128**, 9024; (*b*) Y. Wang, J. Yang, Y.-Y. Liu and J.-F. Ma, *Chem. – Eur. J.*, 2013, **19**, 14591.

8 (*a*) C. Wang, D. Liu and W. Lin, *J. Am. Chem. Soc.*, 2013, **135**, 13222; (*b*) M. D. Rowe, D. H. Thamm, S. L. Kraft and S. Boyes, *Biomacromolecules*, 2009, **10**, 983.

9 (*a*) S. R. Miller, D. Heurtaux, T. Baati, P. Horcajada, J.-M. Grenèche and C. Serre, *Chem. Commun.*, 2010, **46**, 4526; (*b*) I. Imaz, M. Rubio-Martinez, J. An, I. Sole-Font, N. L. Rosi and D. Maspoch, *Chem. Commun.*, 2011, **47**, 7287.

10 (*a*) T. V. Slenters, J. L. Sagué, P. S. Brunetto, S. Zuber, A. Fleury, L. Mirolo, A. Y. Robin, M. Meuwly, O. Gordon, R. Landmann, A. U. Daniels and K. M. Fromm, *Materials*, 2010, **3**, 3407; (*b*) S. R. Miller, E. Alvarez, L. Fradcourt, T. Devic, S. Wuttke, P. S. Wheatley, N. Steunou, C. Bonhomme, C. Gervais, D. Laurencin, R. E. Morris, A. Vimont, M. Daturi, P. Horcajada and C. Serre, *Chem. Commun.*, 2013, **49**, 7773; (*c*) E. Alvarez, A. Garcia-Marquez, T. Devic, N. Steunou, C. Serre, C. Bonhomme, C. Gervais, I. Izquierdo-Barba, M. Vallet-Regí, D. Laurencin, F. Mauri and P. Horcajada, *CrystEngComm*, 2013, **15**, 9899; (*d*) J. Della Rocca, D. Liu and W. Lin, *Nanomedicine*, 2012, **7**, 303.

11 (*a*) D. Sharma, P. Kumar and B. Narasimhan, *Med. Chem. Res.*, 2012, **21**, 796; (*b*) P. Mishra and K. Mishra, *J. Adv. Pharm. Educ. Res.*, 2012, **2**, 110.

12 K. Wang, Y. Yin, C. Li, Z. Geng and Z. Wang, *CrystEngComm*, 2011, **13**, 6231.

13 (*a*) T. V. Slenters, I. Hauser-Gerspach, A. U. Daniels and K. M. Fromm, *J. Mater. Chem.*, 2008, **18**, 5359; (*b*) M. Berchel, T. L. Gall, C. Denis, S. L. Hir, F. Quentel, C. Elleouet, T. Montier, J.-M. Rueff, J.-Y. Salaun, J.-P. Haelters, G. B. Hix, P. Lehn and P.-A. Jaffes, *New J. Chem.*, 2011, **35**, 1000; (*c*) A. M. Kirillov, S. W. Wieczorek, A. Lis, M. F. Guedes da Silva, M. Florek, J. Król, Z. Staroniewicz, P. Smoleński and A. J. L. Pompeiro, *Cryst. Growth Des.*, 2011, **11**, 2711; (*d*) L. Xing, Y. Cao and S. Che, *Chem. Commun.*, 2012, **48**, 5995.

14 L. M. Plum, L. Rink and H. Haase, *Int. J. Environ. Res. Public Health*, 2010, **7**, 1342.

15 J. R. Schwartz, R. G. Marsh and Z. D. Draelos, *Dermatol. Surg.*, 2005, **31**, 837.

16 C. Charnock, B. Brudeli and J. Klaveness, *Eur. J. Pharm. Sci.*, 2004, **21**, 589.

17 J. E. Wolf Jr., N. Kerrouche and S. Arsonnaud, *Cutis*, 2006, **77**, 3.

18 (*a*) A. Katsambas and C. Dessinioti, *Dermatol. Ther.*, 2008, **21**, 86; (*b*) S. Purdy and D. Deberker, *Clin. Evid.*, 2008, **5**, 1714; (*c*) W.-I. Worret and J. W. Fluhr, *J. Dtsch. Dermatol. Ges.*, 2006, **4**, 293.

19 D. M. Thiboutot, A. B. Fleischer Jr., J. Q. Del Rosso and K. Graupe, *J. Drugs Dermatol.*, 2008, **7**, 541.

20 (*a*) K. U. Schallreuter and J. M. Wood, *Cancer Lett.*, 1987, **36**, 297; (*b*) K. Addo-Boadu, J. Wojta, G. Christ, P. Hufnagl, H. Pehamberger and B. R. Binder, *Cancer Lett.*, 1996, **103**, 125.

21 N. J. Lowe, D. Rizk, P. Grimes, M. Billips and S. Pincus, *Clin. Ther.*, 1998, **20**, 945.

22 S. Farshi, *J. Cosmet. Dermatol.*, 2011, **10**, 282.

23 R. A. Bojar, A. G. Cutcliffe, K. Graupe, W. J. Cunliffe and K. T. Holland, *Br. J. Dermatol.*, 1993, **129**, 399.

24 J.-L. Hodeau, P. Bordet, M. Anne, A. Prat, A. N. Fitch, E. Dooryhee, G. Vaughan and A. Freund, *Proc. SPIE*, 1998, **3448**, 353.

25 *Topas V4.2: General Profile and Structure Analysis Software for Powder Diffraction Data*, Bruker AXS Ltd, 2008.

26 A. Altomare, M. C. Burla, M. Camalli, B. Carrozzini, G. L. Cascarano, C. Giacovazzo, A. Guagliardi, A. G. G. Moliterni, G. Polidori and R. Rizzi, *J. Appl. Crystallogr.*, 1999, **32**, 339.

27 E. Capristo, G. Mingrone, A. De Gaetano, G. Addolorato, A. V. Greco and G. Gasbarrini, *Clin. Chim. Acta*, 1999, **289**, 11.

28 CLSI, Clinical and Laboratory Standards Institute: Performance Standards for Antimicrobial Susceptibility Testing: Fifteenth Informational Supplement M100-S15, in *Performance Standards for Antimicrobial Susceptibility Testing: Fifteenth Informational Supplement M100-S15*, Wayne, PA, USA, 2005.

29 C. Livage, C. Egger, M. Nogues and G. Férey, *C. R. Acad. Sci. Paris Chimie*, 2001, **4**, 221.

30 (*a*) J.-S. Kim, H. Kim and M. Ree, *Chem. Mater.*, 2004, **16**, 2981; (*b*) P. J. Saines, P. T. Barton, P. Jain and A. K. Cheetham, *CrystEngComm*, 2012, **14**, 2711.

31 BBLTM Mueller Hinton II Broth (Cation-Adjusted) (accessed December 2013): http://www.bd.com/ds/technicalCenter/inserts/L007475(12)(201102).pdf.

32 Penn State Department of Chemistry (accessed December 2013): http://research.chem.psu.edu/brpgroup/pKa_compilation.pdf.

33 M. H. Kaye and W. T. Thompson, *Uhlig's Corrosion Handbook*, John Wiley & Sons, Hoboken, 2011.

34 K. M. L. Taylor-Pashow, J. Della Rocca, Z. Xie, S. Tran and W. Lin, *J. Am. Chem. Soc.*, 2009, **131**, 14261.

35 (*a*) M. Huang, H. T. Wang, J. X. Chen, Z. B. Wang, J. Y. Sun, D. Y. Zhao and Y. S. Yan, *Microporous Mesoporous Mater.*, 2003, **58**, 105; (*b*) S. S. Kaye, A. Dailly, O. M. Yaghi and J. R. Long, *J. Am. Chem. Soc.*, 2007, **129**, 14176; (*c*) S. Hausdorf, J. Wagler, R. Mossig and F. Mertens, *J. Phys. Chem. A*, 2008, **112**, 7567.

36 (*a*) J. Yang, A. Grzech, F. M. Mulder and F. J. Dingemans, *Chem. Commun.*, 2011, **47**, 5244; (*b*) J. G. Nguyen and S. M. Cohen, *J. Am. Chem. Soc.*, 2010, **13**, 4560.